Bridging Molecular-Scale Interfacial Science with Continuum-Scale Models

Anastasia G. Ilgen*[1], Eric Borguet[2], Franz M. Geiger[3], Julianne M. Gibbs[4], Vicki H. Grassian[5], Young-Shin Jun[6], Nadine Kabengi[7], James D. Kubicki[8]

1. Geochemistry Department, Sandia National Laboratories, USA
2. Department of Chemistry, Temple University, USA
3. Department of Chemistry, Northwestern University, USA
4. Department of Chemistry, University of Alberta, Canada
5. Department of Chemistry & Biochemistry, University of California, San Diego, USA
6. Department of Energy, Environmental & Chemical Engineering, Washington University in St. Louis, USA
7. Department of Geosciences, Georgia State University, USA
8. Department of Earth, Environmental & Resource Sciences, The University of Texas at El Paso, USA

Corresponding author: agilgen@sandia.gov

Abstract: Solid–water interfaces are crucial for clean water, conventional and renewable energy, and effective nuclear waste management. However, reflecting the complexity of reactive interfaces in continuum-scale models is a challenge, leading to oversimplified representations that often fail to predict real-world behavior. This is because these models use fixed parameters derived by averaging across a wide physicochemical range observed at the molecular scale. Recent studies have revealed the stochastic nature of molecular-level surface sites that define a variety of reaction mechanisms, rates, and products even across a single surface. To bridge the molecular knowledge and predictive continuum-scale models, we propose to represent surface properties with probability distributions rather than with discrete constant values derived by averaging across a heterogeneous surface. This conceptual shift in continuum-scale modeling requires exponentially rising computational power. By incorporating our molecular-scale understanding of solid–water interfaces into continuum-scale models we can pave the way for next generation critical technologies and novel environmental solutions.

1. Introduction

Solid–water interfaces play critical roles in engineered systems[1-3] and natural environments.[4] Communication among scientists and engineers working at molecular, microscopic, field, and global scales should be augmented *via* integrated collaborations that seek to add chemical insights into large-scale problems where current assumptions and approximations lead to large uncertainties in predictive models.[5] We lay out a perspective about how to establish such a collaboration that infuses molecular details into larger scale models, including often-used surface complexation (SCM) and reactive transport models (RTM). We propose the development of a new approach for incorporating the vast database of molecular knowledge into continuum-scale models by shifting the model parameterization paradigm. We suggest a conceptual shift in how surface properties are represented from the current state of using discrete values to probability distributions, allowing to reflect real heterogeneities of surfaces. Surface site acidities, charge densities, solvation energies, reaction rates, and solubility constants should be described as probability curves to reflect the interfacial complexity.

Scientists who develop detailed molecular descriptions of solid–water interfaces face a four-fold challenge: (1) interfacial chemistry evolves in complex ways as it is dynamically coupled to the compositions of both the solid and the aqueous phases yet is distinct from either; (2) the number of atoms present at the surface is dwarfed by the number of atoms that compose the bulk phases, thus complicating the deconvolution of surface analytical signals from those of the bulk; (3) real-world interfaces are inherently heterogeneous down to the micro-, nano-, and molecular-scales, making it difficult to build continuum-scale predictive models that capture this complexity and reconcile distinct surface structures with observed net reactivities; and (4) environmental processes span femtosecond to millennia timescales, not always accessible for experimental, analytical, and

computational inquiries. Despite these challenges, previously obscure details of surface reactions are becoming increasingly understood. However, the current numerical tools available for translating interfacial processes into continuum-scale models that describe mm- to km-scale systems are lacking mathematical frameworks for incorporating the wealth of molecular details that have been discovered in the last few decades.

Because of these limitations, scientists who construct SCMs and RTMs often use "average" values to describe the structures and reactivities of solid–water interfaces to reflect relevant molecular information. SCMs are developed to specifically describe ion adsorption behaviors at solid–water interfaces to match either adsorption isotherms or pH-dependent adsorption data (*i.e.*, adsorption edges). The basic schematic for three types of commonly used SCMs is shown in **Figure 1** (reproduced from Ref [6]). These SCMs are based on various continuum-scale models of interfacial structure such as: (*1*) the constant capacitance model (CCM), (*2*) the diffuse layer model (DLM), and (*3*) the triple layer model (TLM). Each of these SCMs assumes that the total free energy of ion adsorption is a sum of chemical adsorption energy (ΔG_{chem}) and Coulomb static energy (ΔG_{coul}), where ΔG_{coul} is directly proportional to the surface potential (ψ) and the charge of the adsorbing ion.[6] In the sections below we illustrate that neither ΔG_{chem} nor ΔG_{coul} can be considered constants in any given interfacial system because of the variability of surface structures that define local surface charge or the reactivity of isolated surface groups, which should lead to variability in the surface potential across the same surface caused by intrinsic surface heterogeneity. Therefore, to reflect the true complexity, ΔG_{chem} and ΔG_{coul} would be best represented by a distribution of values, rather than a fixed value.

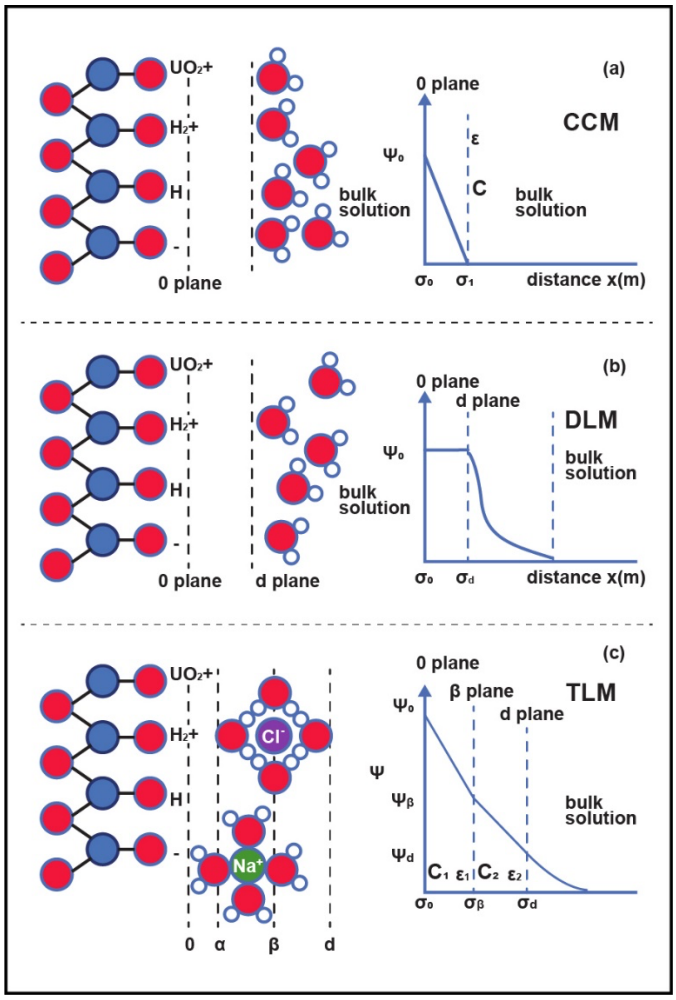

Figure 1. Surface complexation modeling based on (a) Constant capacitance model (CCM); (b) Diffuse layer model (DLM); and (c) Triple layer model (TLM). A *0*-plane in these models limits the solid's surface, a *β*-plane terminates the plane where counter-ions are tightly bound at charged surfaces (Stern layer) and a *d*-plane cuts through the center of the diffuse layer near surfaces. *C*, including C_1 and C_2, denote individual layer capacitance values; ψ is the surface potential corresponding to one of the planes, and σ, including σ_β and σ_d, is charge of the corresponding layers, where σ_0 is charge of the *0*-plane (surface charge, or surface charge density); ε is the dielectric constant or permittivity of the media. Figure adapted with permission from Ref.[6]

To illustrate the sensitivity of a common SCM to input parameters, we calculated the Gouy-Chapman Stern (GCS) potential as a function of Stern layer thickness, *d*, which varies due to spatial heterogeneity of a surface (**Figure 2**). A two-fold change in *d* would result in a factor of two difference in the potential drop across the Stern layer as $\Delta\Phi_{Stern} = \sigma/C$, where σ is the surface charge density and *C* is the capacitance equal to $\varepsilon_r\varepsilon_0/d$ (ε_r and ε_0 are the permittivity of the solution

and of the vacuum, respectively). The resulting change in the electric field in the Stern layer ($-d\Phi/dz$) would then vary accordingly. Opening the expression for the Stern layer potential drop to allow for spatial variations in all three parameters (σ, ε_r, and d) will result in variations of the potential across the electric double layer (EDL). It is reasonable to expect that each of these parameters varies by up to a factor of two (for the surface charge density and Stern layer thickness) and by ten (for the relative permittivity). A sensitivity analysis of the ionic strength dependent Gouy-Chapman Stern potential in terms of physically feasible variations in charge density and Stern layer relative permittivity shows that variations of serval hundred mV occur, owing, for instance, to doubling the charge density and halving the Stern layer permittivity (**Figure 2**). In contrast, doubling both parameters results in only minor potential differences (**Figure 2**). We conclude that expected spatiotemporal variations in the surface charge density and the Stern layer relative permittivity will result in spatiotemporal variations in the surface potential, and the associated electric field, in the range up to several hundred mV. This simple example is directly applicable to other important parameters in mean field or surface complexation models, including the Stern layer thickness, as alluded to above, and further justifies the proposed probabilistic approach to continuum-scale modeling.

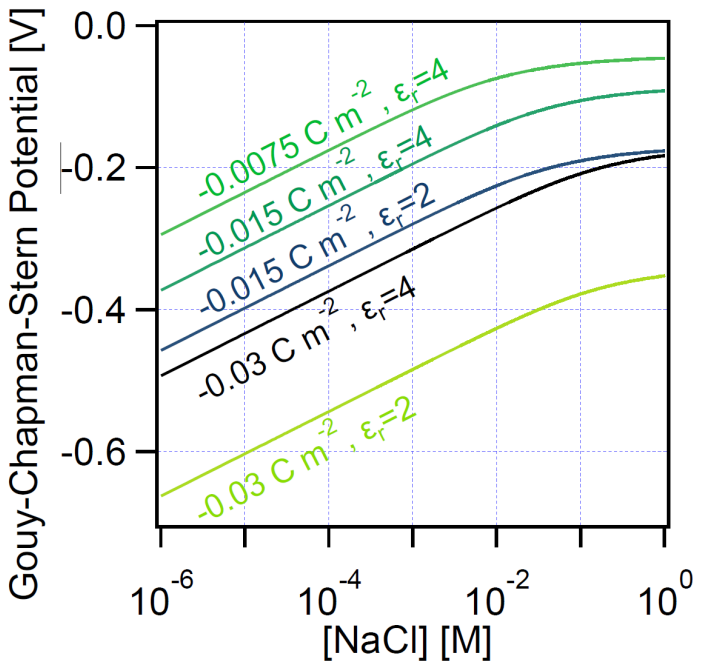

Figure 2. Calculated variability in the ionic strength dependent Gouy-Chapman Stern (GCS) potential due to variations in charge density and Stern layer relative permittivity commonly observed across surfaces. The resulting Gouy-Chapman Stern potential variations reach several hundred mV when doubling the charge density and halving the Stern layer permittivity. In contrast, doubling both parameters results in only minor potential differences.

Furthermore, conventional SCMs describe surface properties and reactivities with a single surface acidity constant and surface complexation constant for a given surface and adsorbate (the more advanced SCMs may go as far as to incorporate two- or three-site models with distinct acidity and/or complexation constants). However, new experiments consistently show that nominally similar surface sites (*e.g.*, Si-OH, see Bañuelos et al.)[7] have vastly different reactivities, which are defined by multiple factors: surface structure, hydrogen bonding in adjacent solution, the surface neighbor species, and aqueous composition. Because continuum-scale simulations rely on empirically fit coefficients to approximate parameter values, they often do not capture experimentally measured outcomes. As we will show below, the mismatch in predicted *vs.* experimentally determined parameters can span orders of magnitude.

138 The other types of continuum-scale reactive models, which are often utilized in important
139 applications such as nuclear waste storage, are reactive transport models (RTMs) that couple
140 transport equations with chemical reactions, including equilibrium constants and kinetic rate laws.
141 Similar to SCMs, equilibrium constants for reactions that are used in RTMs do not fully reflect the
142 reality of a solid–water interface, where isolated surface sites can have dramatically different
143 reactivities. Furthermore, to model the dissolution of solid phases in RTMs average rates or rate
144 constants are selected,[8,9] whereas experimental evidence indicates that the *effective* dissolution rate
145 consists of contributions from specific surface sites, where the rates are vastly different.[10] Because
146 surface structure is dynamic, rates may also vary with time,[11] with reaction Gibbs free energy,[12]
147 and with flow rate.[13] Accordingly, reaction rates may vary several-fold for the same crystalline
148 solid, depending on the molecular, crystallographic, and topographic details of their surfaces that
149 change dynamically in time. Therefore, reaction rates are best described by distributions of
150 possible/probable values and not by a singular discrete number.

151 This Perspective argues that, in place of ensemble averaged constants as input parameters,
152 *probability distributions* are needed to formalize chemical phenomena at interfaces to reflect their
153 heterogeneous nature in SCMs, RTMs, and other continuum-scale models. Current state-of-the-art
154 modeling approaches apply homogeneous chemistry concepts to heterogeneous systems, limiting
155 their applicability and predictive power. A probabilistic approach that captures the stochastic
156 nature of surface sites offers a path forward to bridge detailed molecular-scale information with
157 the continuum-scale models of complex systems. We will show that using probability distributions
158 is appropriate for representing the "surface landscape", (*i.e.,* the stoichiometry of surface sites,
159 surface charge distributions, and surface topologies), as well as equilibrium constant values and
160 reaction rates. This approach provides a new paradigm that we hypothesize will create a more

161 robust predictive power in continuum-scale models by capturing the wealth of molecular-scale
162 information that is increasingly available for interfacial systems. Using molecular-scale
163 information in continuum-scale simulations will advance our capability to model environmental
164 fate and transport, soil system evolution, and to elevate the design and optimization of
165 electrochemical and catalytic processes, desalination membranes, and carbon- and ion-selective
166 capture materials. Achieving this probabilistic approach requires not just advancements in the
167 capabilities of SCMs and RTMs, but also the continued efforts of experimentalists and
168 computational chemists to elucidate molecular details and reactivities of solid−water interfaces.

169 2. Molecular details matter

170 In this section we will illustrate that a surface is not one reactant but instead a combination of
171 different reactants that are distinct, interdependent, and changing. Recent scientific advances have
172 led to molecular descriptions of interfaces of specific solid–water systems that challenge
173 traditional mean-field models of charged surfaces (see Bañuelos et al. for comprehensive review).[7]
174 These studies highlight that molecular details matter as surfaces are heterogeneous at the
175 molecular-scale and cannot be conceptualized as a single "reactant" in interfacial chemistry
176 descriptions. The selected advances illustrated here have been facilitated by new capabilities in
177 scanning probe, synchrotron-based X-ray, and nonlinear optical techniques that reveal the different
178 detailed aspects of the interface under *in situ* conditions in real-time. Furthermore, computational
179 simulations using density functional theory (DFT) and *ab initio* and classical molecular dynamics
180 (MD) have been critical in uncovering reaction mechanisms at solid–water interfaces, helping to
181 interpret experimental observables and distinguish the reactivities of different surface sites. These
182 studies have shown that surface sites can have stark differences in their reactivities, such as acidity
183 and surface complexation reactions. Importantly, the surface site reactivity also depends on the

184 local environment, *i.e.,* the reactivity of the same surface site differs depending on the structure
185 and identity of its immediate neighbors.

186 In the last decade, nonlinear optical methods have greatly enhanced our ability to garner
187 molecular information on buried interfaces, *i.e.*, those surfaces under aqueous solutions. Phase-
188 sensitive measurements have yielded complex spectra generated at solid–water interfaces
189 resolving the orientation of the molecules that contribute to the measured response.[14,15] Moreover,
190 theoretical frameworks used to interpret these measurements now separate the contributions from
191 different regions of the interfacial solution layers and assign them to molecules immediately at the
192 buried surface and those at a distance that are still structurally distinct from molecules in the bulk
193 aqueous phase (the diffuse layer).[15,16] These methods and related approaches have uncovered the
194 details of hydrogen-bonding networks of water immediately adjacent to a surface (in the Stern
195 layer) and how they are perturbed by changes in pH[17] and the addition of aqueous ions.[18] Phase-
196 sensitive measurements have allowed also for the total potential to be quantified directly at the
197 surface.[19] This new capability is important, because the surface potential (ψ) is one of those
198 approximated quantities that must be incorporated into SCMs (**Figure 1**). This quantity is often
199 calculated from mean-field models and rarely had been measured experimentally. Now, the surface
200 potential, which differs from the more commonly measured zeta potential, can be ascertained
201 optically, and at arbitrary ionic strength, using heterodyned second harmonic generation (SHG)[19]
202 as well as synchrotron-based X-ray photoelectron spectroscopy (XPS) albeit under more limited
203 conditions.[20] This ability to measure the total surface potential provides an important experimental
204 benchmark for the widely-used mean-field models for calculating surface potentials and applying
205 the electrokinetic methods used to quantify interfacial potentials. Ultimately, our ability to assess
206 the electrostatics at the surface without having to invoke classic mean-field models, which often

207 rely on semi-empirical parameters and primitive ion models that were put forth based on less
208 sensitive techniques decades ago, will be critical to develop the next generation of surface models
209 and extend them into SCMs and RTMs.

210 Advanced techniques for measuring ψ at oxide surfaces still provide an average value for a
211 given interface. However, we know that charged sites on oxide surfaces are localized resulting
212 from protonation and deprotonation of surface hydroxyls. Whether charges are localized or
213 delocalized significantly impacts both the ion distribution and the net water orientation in the
214 interfacial region according to simulations of charged solid–water interfaces.[21] Specifically, charge
215 localization results in ion accumulation at an interface and local re-orientation of water molecules
216 at interfaces compared with the delocalized charged aqueous interface. Furthermore, recent work
217 using Stark spectroscopy indicates that the local fields can vary significantly across the solid–water
218 interface and that interfacial molecules "sample" this heterogeneous, dynamic environment.[22]

219 The interfacial charge structure can be changed drastically by high salinity. Lee *et al.*[23]
220 observed the salinity-dependent electric double layer (EDL) structure evolution in RbI or RbCl
221 with negatively charged mica surfaces using element-specific resonant anomalous X-ray
222 reflectivity. They found that cations and anions formed alternating discrete layers, causing
223 nonclassical charge overscreening (also referred to as charge reversal) at high salinity. At the silica
224 surface, the impact of overscreening induced by divalent ions with increasing pH on both the water
225 structure and ion speciation within the EDL was also recently observed by Rashwan *et al.* using
226 vibrational SFG (vSFG) and streaming current measurements.[24]

227 Experimental methods capable of mapping out the local structure with molecular-scale
228 resolution are transformative tools for characterizing the chemistry of solid–water interfaces.[7]
229 Scanning probe measurements over nearly atomically flat surfaces, such as mica,[25] paired with

finite-element analysis[26] have yielded topographic information on the molecular-scale of both the interfacial potential and water structure. Such methods have been extended to mapping of organic molecules deposited on metal surfaces.[27] Charge profiling three-dimensional (3D) atomic force microscopy has revealed charge layering of ionic liquids on electrodes at Ångstrom depth resolution.[28] 3D fast-force mapping can also estimate the position of individual water molecules in the Stern layer although this emerging method is complicated by data convolution concerns related to tip-specific effects.[29] Other imaging methods such as transmission electron microscopy (TEM), including scanning (STEM), high-resolution (HRTEM) and liquid cell (*in situ* TEM), in combination with electron energy loss spectroscopy can directly quantify surface structures in dry, humid, or aqueous conditions. Because these measurements are spatially resolved and have near-molecular-scale resolution, they can map out the variety of reactive surface sites on oxide surfaces allowing the abundance of a certain type of surface site to be linked to observable macroscopic reactivities. A well-studied example of this phenomenon is the uptake and release of O_2 by ceria (CeO_2) nanoparticles that are widely used in catalysis and other applications. Combined TEM and modeling studies for CeO_2 have shown that the energetics of O_2 uptake/release is controlled by (*1*) specific facets (crystallographic orientation), (*2*) oxygen site vacancies produced during Ce^{3+}/Ce^{4+} redox reaction, and (*3*) surface hydration (**Figure 3**, from Sayle *et al*.[30], and Seal *et al*.[2]). Because surface defects often produce high energy reactive sites, the emerging research field of defect engineering for nanomaterials is critically tied to these new high-resolution measurements.

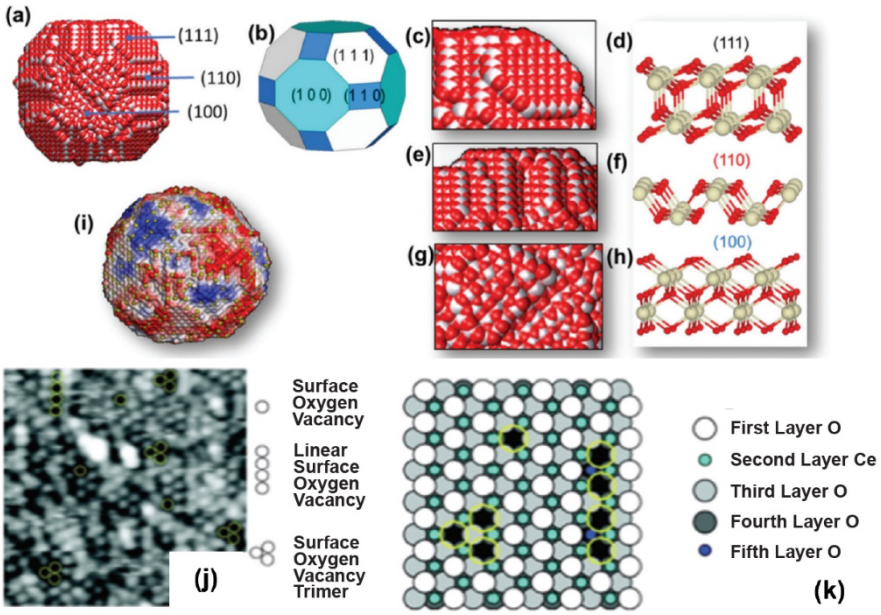

Figure 3. Surface structures of ceria (CeO_2) nanoparticles. (a) Full atom level model of CeO_2 nanoparticle; (b) Schematic of CeO_2 nanoparticle showing crystallographic surfaces; (c) Enlarged view of the CeO_2 (111) surface showing the presence of surface steps and corners; (d) Perfect (111) surface of CeO_2 crystal; (e) Nanostructured (110) surface; (f) Perfect (110) surface; (g) Nanostructured (100) surface; (h) perfect (100) surface. Ce = white, O = red; (i) Visualization of catalytic activity of a CeO_2 nanoparticle surface, where oxygen atoms are colored by their lability—the energetic cost of their removal from the surface. Red-white-blue gradient scale, where red corresponds to labile oxygen (energetically easy to extract) and blue corresponds to oxygen ions that are difficult to extract. The yellow spheres are Ce^{3+} species; (j) Scanning tunneling microscopy image of CeO_2 surface; (k) corresponding structural model. Adapted with permission from Seal *et al*.[2]

Inevitably, the observed heterogeneities of the surface structures discussed above lead to variability in surface properties, such as interfacial potentials, acidities of surface groups (pK_a values),[31-33] dissolution rates,[10] surface speciation, ion jamming with observed hysteresis in surface acid-base chemistry,[33,34] and heterogeneous nucleation patterns across a single surface.[35,36] Further complicating the situation is the recognition that the surfaces of some materials, *e.g.*, SiO_2, can have *localized* hydrophilic and hydrophobic regions[36-38] that have been proposed to produce different surface acidity constants[39] in concert with changes in hydrogen bonding effects on the distribution of silanol site acidities.[40]

Capturing the acidity of surface groups is of specific interest to SCM and RTM development because site charge influences surface reactivity and may vary greatly on the same surface.[41-43] A recent significant and surprising finding by Wagner *et al.*[41] who combined non-contact AFM measurements and DFT modeling indicates that surface hydroxyl groups at an In_2O_3 (111) surface have pK_a values varying several orders of magnitude, based on the H-bond strength measurements at individual surface sites (**Figure 4**). Multiple distinct pK_a values have also been observed for silica in both theory and experiment under aqueous conditions.[31,39,40] Therefore, the relative abundance of different sites varies significantly, which we propose should be represented as a probability curve in continuum models.

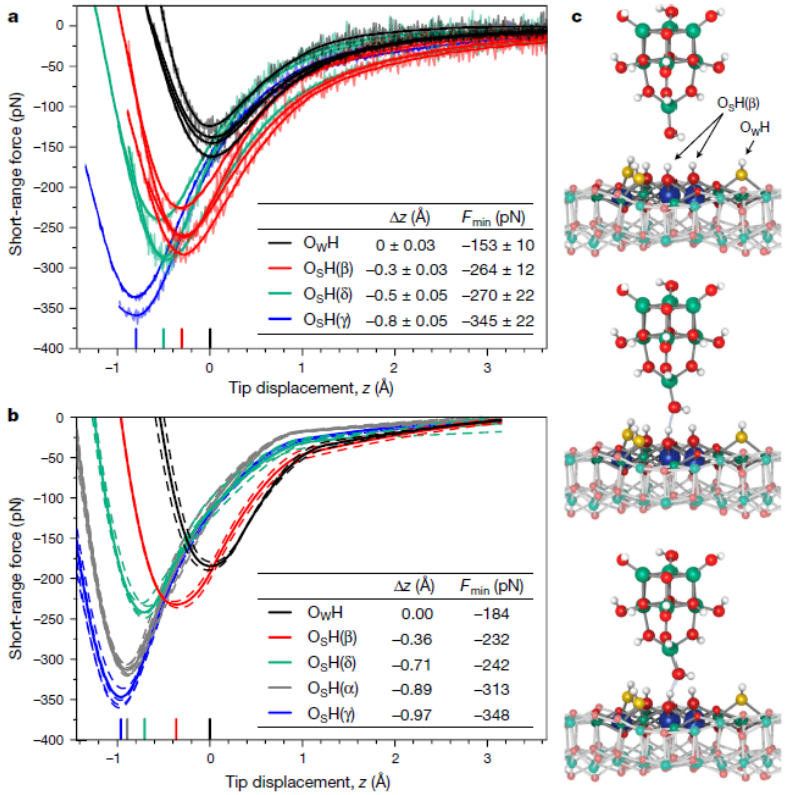

Figure 4. Probing individual hydroxyls on In_2O_3 surface with an Atomic Force Microscopy tip. (a) Experimental short-range force–distance curves for the OH groups; (b) Calculated short-range force–distance curves for the OH groups. Adapted with permission from Wagner *et al.*[41]

Although imaging surface structures, localized surface potentials, local pK_a values, and particle–particle interactions are paramount to understanding these systems, it is equally crucial to capture time-dependent fluctuations referred to as surface dynamics. Most environmental interfaces are intrinsically dynamic and sensitive to changes in pH and the presence of ions as they consist of amphoteric sites that become charged and interact, either in a specific or non-specific manner. Generally, models consider that a given solid will exhibit a trend in affinity towards ions based on its composition. Yet, recent experimental work for the planar[44,45] and nanopore silica–water interfaces[46] reveals that such trends in ion affinity can be significantly altered as the pH is changed. One hypothesis that can qualitatively explain a change in relative ion affinity is that the ions can interact with at least two distinct sites on the silica surface, one charged and one neutral, and as the relative ratio of charged to neutral sites increases with pH so does the affinity for ions in solution.[45] Current work aims to investigate whether revising SCMs to include two-site binding of cations can capture such pH-dependent trends in ion affinities. Furthermore, changes in pH, ion concentrations, and solid chemistries might reveal that a probabilistic approach capturing distributions of affinities, rather than two affinity constants, can better predict such behavior.

Real-world solid–water interfaces must also contend with dynamic chemical and geometric complexities: the composition of the aqueous phase at the solid–water interface is multi-component where competitive adsorption plays an important role in Stern and diffuse layer structures.[47] Continuum-scale models must capture the dynamics and coupled behavior between adsorbates, water, and surface site structures. Furthermore, nanoconfinement of surfaces often leads to anomalous chemistry where interfacial reactivity is dictated by the spatial dimension of the reactive solid–water interface.[42,48,49] In particular, in nanopores, the polarization force between ions and the solid surface at an interface determines ion propensity toward nanoconfined spaces.[49]

Capturing interfacial reactivity is further complicated by the fact that the speciation of adsorbed ions, and likely of surface sites,[50] can vary with ionic strength and surface coverage. For instance, several classic linear and nonlinear optical measurements as well as atomistic simulations have shown that surfaces functionalized with carboxylic acids remain neutral (uncharged) even at highly basic pH values.[51-53] The underlying mechanism is one in which Coulomb repulsion within the surface plane is largely reduced when the carboxylate groups pick up a proton from the aqueous solution to form carboxylic acid dimers, similar to those found in glacial acidic acid (an insulating liquid). A similar phenomenon might be occurring for bare oxides such as silica where a bimodal distribution of acidities has been observed for silanol sites above the point-of-zero-charge.[31-33] Likewise, Sr^{2+} as well as some lanthanide cations (nominally 3+ in solution) exist as singly-charged species when they are absorbed to certain surfaces.[54,55] In this case, the underlying mechanism likely involves replacing a water molecule from the ion's hydration sphere with a counter-ion, such as chloride or surface deprotonation to create an OH^- group.[56,57] Sr^{2+} then absorbs as the $[SrCl]^+$ ion pair, which is subject to reduced lateral Coulomb repulsion. SCMs should take this effect into account, but currently do not. This is a problem of exponential sensitivity, as the Boltzmann term governing the surface coverage is raised to the power of the charge of the adsorbed ion. If this charge changes from 3 to 2 or from 2 to 1, the exponential sensitivity indicates a much different surface coverage relative to what is expected from bulk thermodynamics. We note that such ion-pairing effects are routinely observed in brine solutions (NaCl > 1 M),[58] but they occur at surfaces when electrolyte concentrations are orders of magnitude smaller compared to brines, for example at the fused silica/water interface Sr^{2+}–Cl^- ion pairing occurs once NaCl concentration reaches only 10 mM. The surface-promoted ion-pairing processes need to be incorporated into

new descriptions of Stern layer for ion speciation. When RTMs solve for chemical speciation, they do not incorporate surface-promoted shifts in speciation as described here.

The presence of salts (electrolytes) can influence solid–water interactions, including surface complexation, dissolution, and precipitation reactions. Since the work of Dove[59] and coworkers on silica dissolution, researchers have attempted to further unravel the details of salt effects on solid–water interfaces. For example, Icenhower and Dove[60] found that dissolution rates can increase by over 20 times in 0.05 M NaCl solution compared to de-ionized water. Notably, the same experiments show that the activation energy (74.5 ± 1.4 kJ mol^{-1}) in the range of 25 to 250°C does not change within experimental error with this increase in rate constant. This suggests that the Arrhenius pre-exponential factor (A) related to the activation entropy of the reaction is changing rather than the activation enthalpy. Kubicki *et al.*[61] hypothesized, based on DFT-MD simulations, that the dissolution entropy is made more favorable when salts are present at the interface due to changing H-bonding that favors intra-surface H-bonds and thus H^+-transfer and hydrolysis of Si–O–Si linkages leading to dissolution. This observation of H-bonding changes is consistent with vSFG experiments by Rehl *et al.*,[18] revealing the decrease in ordered water in the Stern layer at the silica surface upon salt addition. Likewise, Dewan *et al.*[62] showed that salt impacts structured interfacial water most significantly near neutral pH where the effect of salt on accelerating silica dissociation is greatest.[21,62] Other simulations and time-resolved vSFG (TR-vSFG) spectroscopy have found similar behavior with addition of salts.[76,77]

In addition to dissolution, the salt concentrations and types can affect the nucleation of metal (hydr)oxides and their subsequent growth and Ostwald ripening. For example, Li and Jun examined the effect of salinity on $CaCO_3$ nucleation on quartz using grazing incidence small angle X-ray scattering.[63] When salinity increased from 0.15 to 0.85 M NaCl, effective interfacial

energies dropped from 47.1 mJ/m^2 to 36.4 mJ/m^2, thus decreasing the thermodynamic penalty of nucleation. However, the kinetic factor for nucleation (J_0)—related to ion diffusion and nuclei surface properties—reduced ~13 times. Lower J_0 values resulted from slower $CaCO_3$ monomers impingement rate caused by decreased electrostatic attraction at high salinity, which is also consistent with charge overscreening at high salinity. Based on these thermodynamic and kinetic contributions to the $CaCO_3$ nucleation, the net nucleation rates could increase an order of magnitude at higher salinities. Furthermore, as shown in **Figure 5**, the nucleation and growth of iron (hydr)oxide nanoparticles are also controlled by many aqueous solution variables, such as the salinity,[64] types of salt ions, co-existing oxyanions,[65] and natural organic matter.[66] Even with this known complexity, RTMs typically consider solid nucleation process to be instantaneous or start as soon as solution reaches the saturation index for a given phase, and do not count the nucleation step as a discrete part of the process. This oversimplification of nucleation processes can result in discrepancies between experimental findings and RTM results.[67]

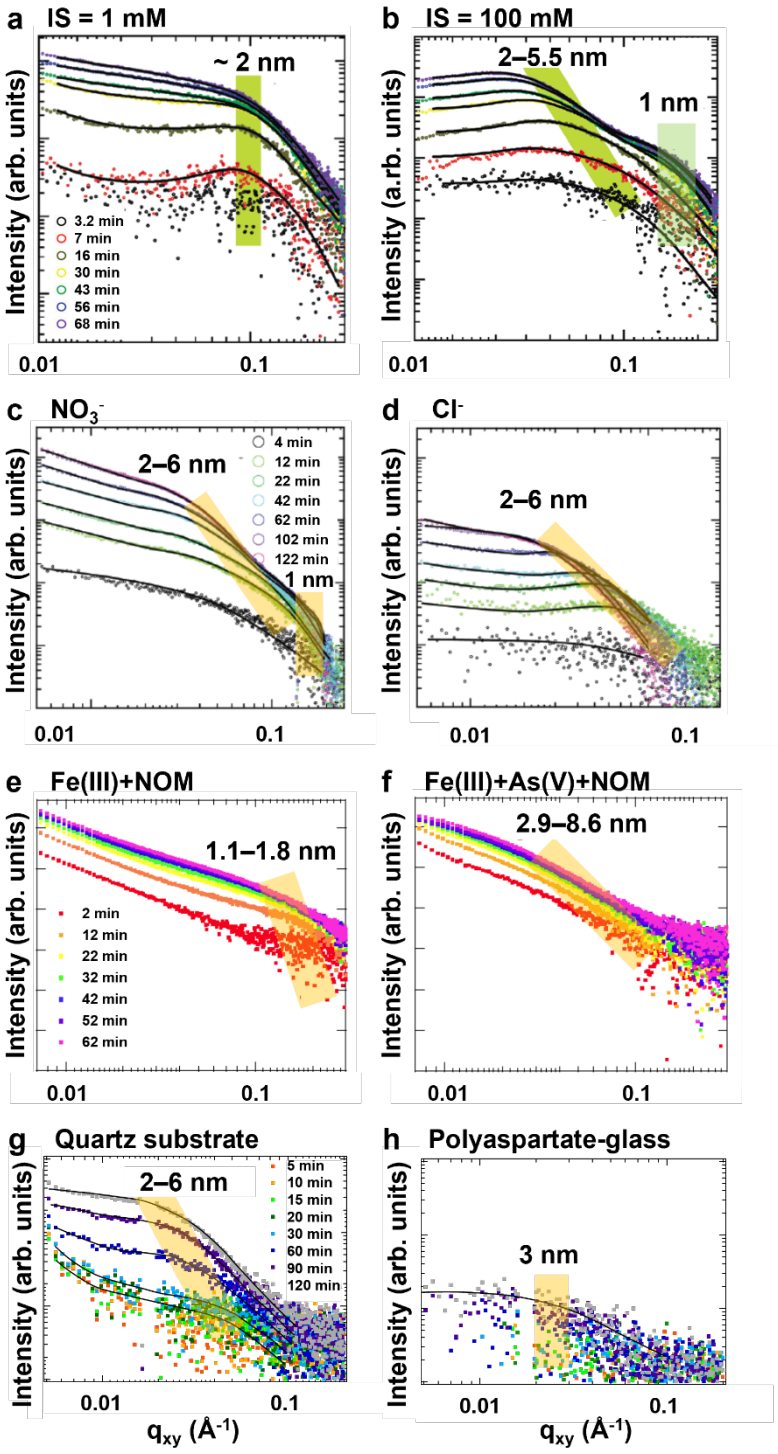

Figure 5. *In situ* measurements of heterogeneous nucleation on quartz substrates in a solution containing 10^{-4} M $Fe(NO_3)_3$ at pH 3.6 ± 0.2 by grazing incidence small angle X-ray scattering (GISAXS), showing in-plane (q_{xy}) 1D scattering. The shaded boxes indicate the particle size evolution with reaction time. Adapted with permission from Jun *et al.* (2016)[36] (a) With 1 mM $NaNO_3$ ionic strength (IS), nucleation is dominant. (b) With 100 mM $NaNO_3$ IS, particles grew from ~2–5.5 nm, with the formation of secondary ~1 nm particles. Detailed discussion about images (a) and (b) is available in Ref. [64] (c) With 10 mM $NaNO_3$, both nucleation and growth were observed. (d) With 10 mM NaCl, although the particle

size is comparable to the nitrate system, the total particle volume does not increase, indicating Ostwald ripening. Detailed discussion about images (c) and (d) can be found in Ref.[68] (e) In the presence of natural organic matter (NOM), particles aggregate, as indicated by power law scattering at low *q*. (f) In the presence of both arsenate and NOM, large particles are also observed. Further discussion about images (e) and (f) is available in Ref.[65]. (g-h) The influence of substrate chemistry is evaluated by coating the surface with hydrophobic polyaspartate. More information about images (g) and (h) can be found in Ref.[66]

As shown above, the chemical complexity of even simple oxide–water interfaces is daunting from a molecular perspective. These surfaces become even more complicated in the presence of organic and microbial communities. Grassian and co-workers have shown that dissolved organic matter can coat oxide surfaces at low and circumneutral pH. [69-73] Moreover, surface adsorption from complex aqueous phase systems containing biomolecules, humic and fulvic substances show that larger complex macromolecules adsorb onto mineral surfaces in a manner that depends on solution pH and ionic strength. Similarly, biological components such as proteins adhere to oxide surfaces to form an "eco-corona"[74] and the protein-oxide surface interactions depend on pH, the nature of the surface and neighboring oxyanions.[69-71] Environmental DNA (eDNA) can attach to oxide particle surfaces but little is known about these interactions and how they impact the underlying surface structure and reactivity as well as the stability of adsorbed eDNA.[75]

These cumulative findings further support two notions: (*1*) interfacial water structure is a key player in interfacial reactivity and (*2*) salt ions are not spectator species at solid–water interfaces. We have shown how surfaces are heterogeneous on all scales of interest, and how interactions with complex molecular species that are typically present in the environment make these systems hard to study. Additionally, in low humidity environments, such as Earth's atmosphere, the surface heterogeneity of single particles can control water adsorption on surfaces as a function of relative humidity.[7,78] Specifically, edge and defect sites adsorb water preferentially from the gas phase as a function of increasing relative humidity prior to the adsorption of water on planar surfaces. The spatially resolved studies, including infrared nanospectroscopy,[78] show how surfaces are

heterogeneous and water does not uniformly coat the surface, meaning that only select surface sites can participate in reactions.

A challenge, as well as an opportunity, moving forward is to utilize the state-of-the-art tools to examine more realistic, chemically/structurally heterogeneous surfaces in complex environments that contain ions, dissolved organic matter and biological components to understand main molecular controls on surface reactivities. We can then test the hypothesis proposed here that describing main reactivity parameters with probability curves leads to more accurate continuum-scale models. Le Traon *et al*.[79] highlights that reaction kinetics in porous systems deviates from the batch experiments by orders of magnitude, demanding that experiments and simulations more realistically capture larger scale effects. This possibility raises several thought-provoking questions such as: *Do aqueous and solid phase complexities produce a heterogeneous surface with different domains? Are the surfaces "patchy" with some hydrophilic and hydrophobic domains, and some regions enriched with adsorbed species (or covered with organic matter)? Can these complex surfaces be described by probabilistic models to capture all types of reactive surface sites for all surface domains?* These are difficult yet important questions to resolve to understand the full chemical complexity of solid–water interfaces in the environment.

In the following Section 3 we will discuss examples where interfacial processes were successfully incorporated into continuum-scale models, as well as those cases where such models cannot be constructed without a complete re-working of the mathematical and statistical approaches on which they are built.

3. Rectifying the Molecular View with Ensemble Models

In this section we will show how mean-field models work in some instances but not in others. To take the heterogeneity of reactive sites during adsorption into account, a commonly used equilibrium adsorption model at a solid–water interface is the Freundlich isotherm, which theoretically accounts for heterogeneous surface sites. Yet only one affinity constant describing bonding strength is derived from adsorption data and this averages the enthalpy of adsorption ΔH_{ads} for all sites. If the range of ΔH_{ads} is narrow, using one constant value would not be a major issue; however, inverse adsorption chromatography,[80] and *operando* flow microcalorimetry have demonstrated that the range of ΔH_{ads} values for the same sorbent–sorbate (surface–ion) pair can be up to 200 kJ mol^{-1}! Thus, one can infer that the variation in ΔH_{ads} is not a simple matter of adsorption reactions at the same type of sites, which is less favorable with increasing sorbate coverage (**Figure 6**). Instead, the ΔH_{ads} variation reflects different types of surface sites with distinct bonding mechanisms, consistent with the notions of local spatial heterogeneity and stochastic distribution of surface reactivities discussed earlier. Many adsorption isotherm studies report better fits to the data at the mid-range of solution concentrations and are less accurate at the low- and high-concentration tails,[81] which is indicative that the values at the higher and lower tails of the probability curve are ignored. Because surface defects likely have the most negative ΔH_{ads} values and lowest surface site densities (representing tail ends of the site probability curve), they have not been modeled accurately. Considering that in many real-world scenarios, the sorbates are present at trace levels, the applicability of models based on ideal surfaces at higher aqueous concentrations that are typically studied in a laboratory setting becomes questionable. There are also critical needs for thermodynamic data and computational chemistry models that can address the lower concentrations and reactions at surface defects[82] and in nanopores[46,49] to obtain predictable thermodynamics and kinetics under realistic environmental conditions.

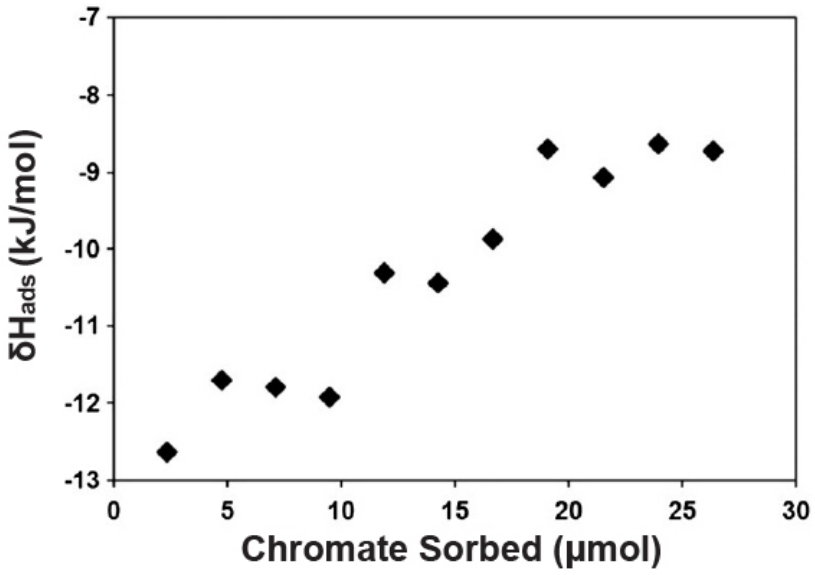

Figure 6. Differential molar enthalpies (δH_{ads}) measured by *operando* flow microcalorimetry for the sorption of chromate on ferrihydrite, showing that the values become less negative (less favorable) with increasing surface loading. Adapted with permission from Kabengi *et al*. [83]

One promising example is the determination of Fe-oxy(hydr)oxide reactive sites that has been translated into a SCM capable of unifying adsorption equilibrium constants for the important contaminant chromate.[84] Bompoti *et al*.[84] utilized the MUSE algorithm and found that in SCMs it was easiest to keep the reactive site densities fixed for each solid and vary the solid concentration and capacitance until the model agreed with experimental data. High resolution data, for example using STEM HAADF helps determine the crystal face contributions for different surface sites, and the respective site densities characteristic for each surface that can be incorporated in SCMs.[85]

When considering larger scales in RTMs, the dynamic evolution of solid–water interfaces can significantly alter the fate and transport of ions, which is not fully captured in current models. Adsorption of chemical species and temporal evolution of solid phases due to dissolution-precipitation processes changes reactive site densities and types. Until recently, RTM could not include solid nucleation due to the lack of experimental information about nucleation. Instead, it captures precipitation as a group term by assuming that nucleation is instantaneous, and only

459 includes the solid's growth rate. RTMs also do not capture pore-size effects on solubility and
460 nucleation kinetics. Recent advances have been made to incorporate experimentally obtained
461 kinetic and thermodynamic information (*e.g.,* nucleation rates, activation energies, and interfacial
462 energies)[63,86,87] of calcium carbonate nucleation into an RTM code CrunchTope. The incorporation
463 of nanoscale interfacial reactions into the RTM improved the model accuracy of both the evolution
464 of the $Ca(OH)_2$-depleted zone and the surface dissolution zone at supercritical CO_2–brine–cement
465 interfaces (**Figure 7**).[67] Experimentally-obtained nucleation thermodynamic and kinetic
466 information are important in scaling up nanoscale observations of chemical reactions to larger
467 scale predictions. Similarly, this improved RTM framework can be utilized to predict managed
468 aquifer recharge (MAR) where reclaimed water is used to replenish underground reservoirs. The
469 reclaimed water for MAR is rich in dissolved oxygen, which can alter the dissolution of minerals
470 with toxic components such as arsenic-bearing iron sulfides and lead to subsequent iron
471 (hydr)oxide nucleation and toxic species adsorption onto the newly formed iron (hydr)oxides.[88-91]
472 Understanding the nucleation and dynamic interfacial chemical processes and incorporating them
473 into RTMs will significantly improve the predictions of pollutant mobility, benefiting safer aquifer
474 management to address water shortage problems.
475

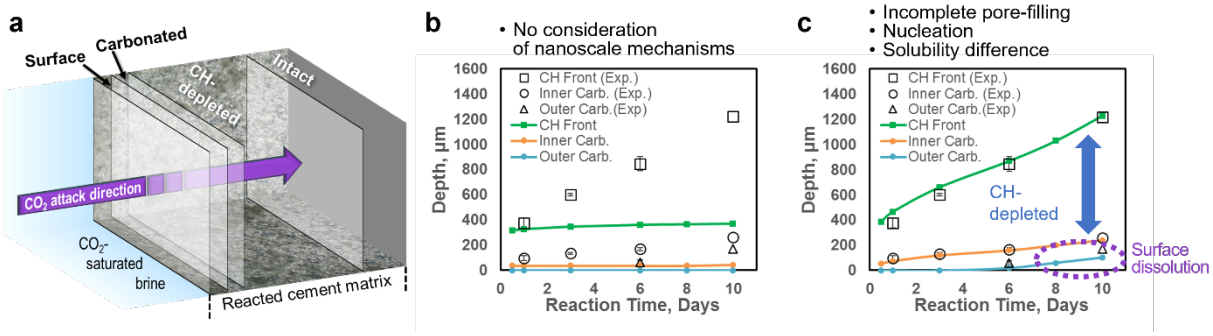

Figure 7. Incorporation of nanoscale interfacial reaction into a reactive transport model. **(a)**. Illustration of direction of CO_2 attack into the cement matrix. The cement samples were reacted in a CO_2-saturated brine (0.5 M NaCl) with a solid-to-liquid volumetric ratio of 1/16. The solution was equilibrated at 95°C under 100 ± 5 bar of CO_2. A total alteration thickness of 1220 ± 90 µm was observed, including a 960 µm CH ($Ca(OH)_2$, portlandite)-depleted zone, a 100 µm carbonated layer, and a 170 µm surface region. Interfaces between zones are drawn to scale. **(b, c).** Modeling results with and without sufficient consideration of nanoscale mechanisms in comparison with experimental data. **(b)** Results with no consideration of nanoscale mechanisms. **(c)** Results with consideration of incomplete filling of pore space at nanoscale, nucleation kinetics, an enhanced solubility in confined pores. By incorporating nanoscale evolution of interfacial chemistry into RTM can generate a better match with experimental observations. Adapted with permission from American Chemical Society from Ref.[67]

4. The Way Forward: Towards Predicting and Controlling Interfacial Behavior

A logical next step for improving the accuracy of continuum-scale models is to increase the number of discrete parameters used in these models (*e.g.*, use two pK_a values instead of one). Such approaches have already been explored and do indeed show increased accuracy.[92] However, should the splitting of single variables into sets of discrete values (multiple-parameter approach) be the way forward? We argue that it should not be, and a paradigm shift is urgently needed. The fundamental question remains—can we keep applying homogeneous chemistry concepts to heterogeneous systems? The probabilistic nature of chemical phenomena in homogeneous systems has been addressed by statistical mechanics—*e.g.,* the Boltzmann distribution describes the physical nature of molecules in populations having different states, the likelihood of which

changes based on the conditions imposed on these populations. Because gaseous or aqueous systems are well-mixed, the Boltzmann distribution is usually Gaussian. When we consider solid surfaces involved in interfacial reactions, a "well-mixed" state is fundamentally impossible for any realistic solid surface. Current molecular models and spatially resolved measurements can capture surface heterogeneity and characterize the localized reactive domains on surfaces at molecular-, nano-, and other scales discussed in **Section 2** of this Perspective. The problem is that the continuum-scale models, such as SCM and RTMs, are not designed to incorporate spatially differing reactivities of surfaces. We propose that probability distributions of surface descriptors instead of average constant values should be used to formalize interfacial properties in continuum-scale models. Therefore, using probabilities to describe surface properties is a more promising approach in comparison to the stepwise increase in the number of variable values used in multi-parameter sets. Including probability distributions for the variables of interest could result in efficient continuum-scale models because localized effects will be incorporated within non-localized parameterization schemes. Hence, this approach has the potential to address surface heterogeneity at different scales. If successful, this new paradigm will lead to scale-independent, universal models that would allow for the prediction of interfacial reactivities in complex chemical systems for the first time, a dream come true for scientists and engineers in many research fields.

To begin, we need to develop new mathematical frameworks and computational approaches to describe chemical parameters and properties as probability distributions, instead of ensemble average values, to reflect real-world complexity and to generate scaled-up SCMs and RTMs. We propose that accounting for chemical and structural complexity in such new generation SCM and RTM codes requires re-writing them using a fundamentally new approach. As shown in our examples above, reaction rates, equilibrium constants, and surface acidity constants vary across a

surface and correlate to distinct structural characteristics (*e.g.*, oxygen vacancies, crystallographic orientation, local structure of amorphous phases, sorbates, and "spectator" ions). We anticipate that normal, bell-shape curves could sufficiently capture the relevant parameter space in some cases where stochastic processes dominate, while in other cases where surface reactivity is a sum of non-random phenomena, they will be best described by more complex types of probability curves. We advocate for applied mathematicians and statisticians to become more involved in interfacial chemistry research to develop rigorous descriptions of interfacial processes for specific use in RTM and SCM codes. The inspiration for such models can be drawn from molecular-scale probabilistic algorithms, including Metropolis Monte Carlo (statistical sampling of energetic states)[93] and Kinetic Monte Carlo (sampling of reaction rates).[94] These models are currently limited to molecular-scales. From the experimental side, approaches that can quantify the spatiotemporal variation of heterogeneous rates, adsorption free energies, as well as interfacial capacitance, relative permittivity in the Stern layer, and distribution of electric fields are needed to inform these models.

In the geoscience community, Lüttge and co-authors proposed using stochastic models to capture mineral dissolution processes.[95-98] This conceptual approach was motivated by high-resolution *in situ* measurements on carbonate and silicate surfaces in aqueous solutions. These measurements clearly indicate site-dependency and time-dependency of the dissolution rates, where the probability distributions evolve in time (**Figure 8**). For calcite surfaces in **Figure 8**, we see that the initial surface topography has a measurable impact on the mean rate values (peaks in the distribution curves) and on the width of the distributions. In fact, a dissolution rate is more accurately represented by a term "rate spectra," given the variability and gradual changes across a

545 given crystalline surface.[10] Importantly, Lüttge *et al.* developed an initial framework for treating
546 dissolution phenomena using a probabilistic approach with the dissolution probability defined as:[98]

547 $$P_i = \prod_{j=1}^{i} P_j \qquad (1)$$

548 Here, P_i is the dissolution probability for a molecule with *i* bonds to the surface written as the
549 product of hydrolysis probabilities over all bonds. Furthermore the logarithm of probability for an
550 individual surface unit to be dissolved is proportional to the sum of activation energies for bond
551 hydrolysis ΔE_{ij}:[98]

552 $$lnP_i = -\frac{\sum_{j=i}^{i} \Delta E_{ij}}{kT} \qquad (2)$$

553 where *k* is the Boltzmann constant, and *T* is temperature. We must note that the variability in the
554 measured dissolution rates shown in **Figure 8** is 2 to 3-fold, because these measurements were
555 conducted on the same crystallographic surface. For numerous solids, the difference in dissolution
556 rates for different crystallographic terminations may reach orders of magnitude. Therefore, for
557 realistic solids the probability weighted approach is crucial, because averaging and ignoring this
558 variability may result in model predictions that are "off" by orders of magnitude.

559 Guren *et al.*[99] illustrate how to derive a set of dissolution rate probabilities from Kinetic
560 Monte Carlo simulations and then how to use them as input into the macroscopic stochastic model.
561 The result of this rigorous procedure is an accurate representation of mineral dissolution that takes
562 place at different surfaces and surface sites of the same material. Regarding RTM, an approach for
563 parameterizing heterogeneity in surface reactivity has been recently demonstrated using
564 nanotopographic images to generate a distribution of surface slope factors that act as a correction
565 factor for the RTM-calculated rates. This approach led to much better agreement between the
566 simulated dissolution rate maps and rate spectra than the standard RTM.[100,101] While these

examples are extremely promising and represent an advance in the field of reaction modeling, the results are still limited to simple systems. A major break-through is needed for translating chemical knowledge from molecular-scale into continuum-scale models.

In this Perspective we propose that an approach that captures probability distributions must be applied in SCMs and RTMs to encompass *all relevant constants and surface properties*, including dissolution rates and nucleation and growth rates, when considering chemistry of solid–water interfaces (**Figure 9**).

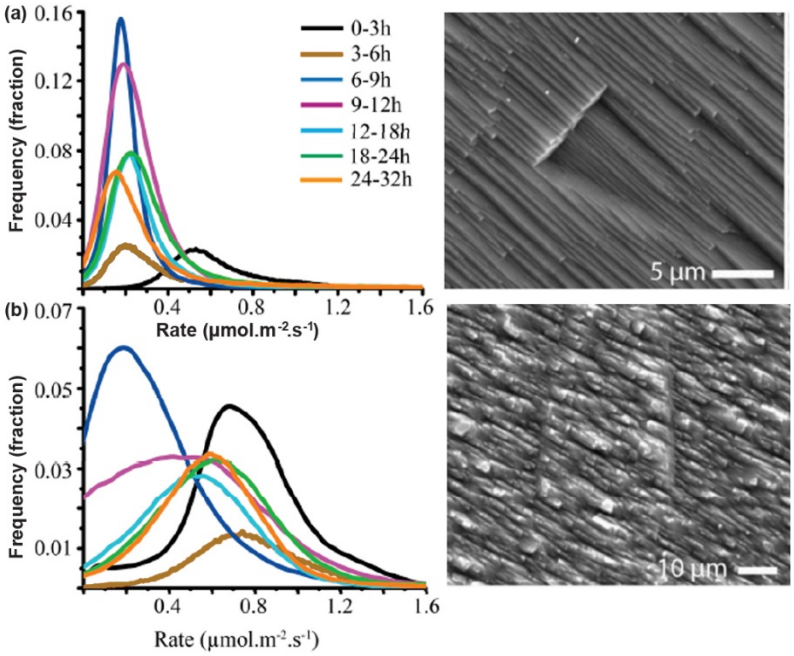

Figure 8. Probability distributions of calcite dissolution rates measured in laboratory dissolution experiments. (a) Dissolution rate spectra for "striated" surface; and (b) Dissolution rate spectra for "hill-and-valley" surface. Adapted with permission from Trindade Pedrosa *et al.*[97]

582 Developing new methods for incorporating probability distributions into SCM and RTM
583 codes for the numerous reactive surfaces present in the environment will be possible by utilizing
584 new computational approaches. A longstanding grand challenge in computational science has been
585 the seamless transfer of information across scales from molecular to field-scales.[102] In practice,
586 this ideal has not been achieved because funding for multi-scale modeling efforts have not been
587 the norm and computational limits have not allowed significant overlap in spatiotemporal scales
588 among the various approaches. The latter obstacle can be overcome with the advent of exascale
589 computing and the development of codes that incorporate machine learning (ML)-based
590 interatomic potentials or ML-IAPs.[103] Connecting atomistic and pore scale simulations through
591 advanced computational power can be achieved by systematic development of interatomic

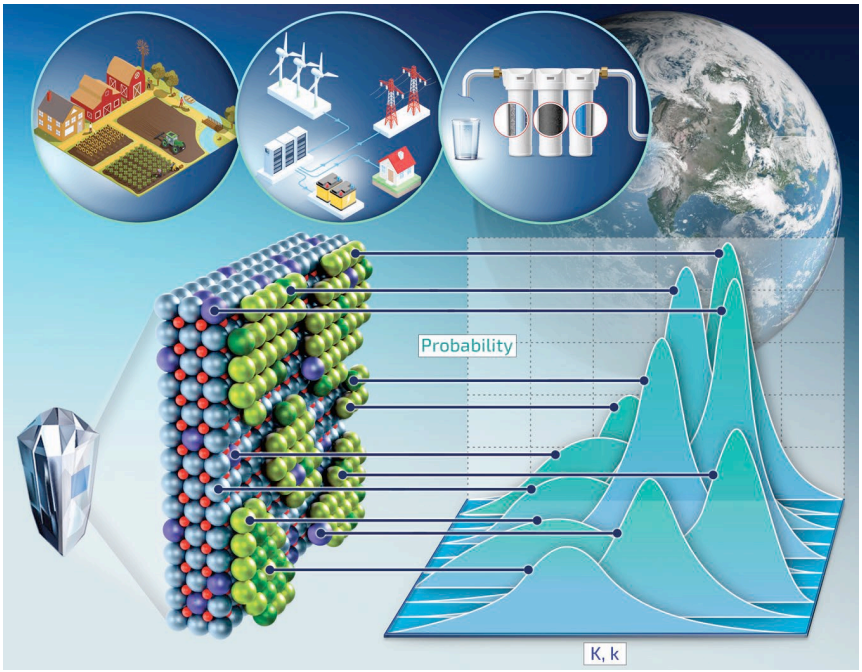

Figure 9. Schematic representation of various surface structures on a single crystal surface that have reactivities best represented by a distribution of equilibrium constants (K) and rection rate constants (k). These dynamic surface reactions include solvation, surface complexation, and attachment-detachment processes due to dissolution or precipitation. Chemistry of solid-water interfaces is crucial for understanding environmental fate and transport, and for applications such as water treatment, conventional and unconventional energy, and agriculture (all of which are represented with symbols in the upper portion of the figure).

592 potentials *via* machine-learning. Exascale computing makes simulations of 10^7 atoms over
593 durations of microseconds possible, and the ML techniques allow for the development of accurate,
594 reactive IAPs based on experimental data and quantum results. Thus, it would be possible to
595 perform atomistic simulations that overlap with the mesoscale and can more realistically represent
596 solid–water interfaces. Exascale computers will allow for accurate atomistic simulations of
597 reactions and flow on scales that overlap the micron-scale elemental volumes of lattice Boltzmann
598 simulations.[104] Coarse-grained mesoscale simulations (*i.e.,* mesoscale) allow for larger and longer
599 spatiotemporal scales that overlap finite element and continuum methods. This "bottom-up"
600 approach can provide parameters that are useful in larger scale models such as SCM (*e.g.,* Fitts *et*
601 *al.*[105]). Additionally, ML can be used to identify feature importance, value clustering, and detecting
602 anomalous values,[106] all of which can aid in the statistical descriptions of interfacial reactivities.
603 Smaller scale simulations can be used to test assumptions and approximations made for larger
604 scale simulations while simultaneously providing chemical mechanism information that could be
605 incorporated into SCMs or RTMs. By incorporating probability distributions and integrating
606 across scales with experiments and simulations, it will become possible to derive new modeling
607 paradigms that are consistent with field observations and incorporate molecular-level information.
608 This approach will enable bridging of laboratory experiments with modeling efforts to predict
609 chemical transformation in complex industrial systems and natural environments, including
610 critical settings such as nuclear waste sites. Similar approaches can be used for predicting catalyst
611 performance and to design fit-for-purpose materials for energy and the environment. With
612 exponentially rising computational power, the advancement in machine learning and artificial
613 intelligence tools and the increasing spatiotemporal resolution of laboratory measurements, this

perspective provides a conceptual framework that could enable sustainable solutions to global problems including clean water, renewable energy, and climate change.

Acknowledgements

We thank M. Rubio and D. Thompson at Sandia National Laboratories for help with graphics design and editing. We are grateful to the three reviewers, who provided valuable feedback for the proposed concept. AGI was supported by the U.S. Department of Energy, Office of Science, Office of Basic Energy Sciences, Chemical Sciences, Geosciences, and Biosciences Division under Field Work Proposal Number 23-015452. EB gratefully acknowledges the support of the National Science Foundation (CHE 2102557). FMG was supported by the US National Science Foundation (CHE- 2153191) and the Department of Energy (DE-SC0023342). VHG was funded in whole or in part by the Army Research Office/Army Research Laboratory via grant W911NF-23-1-0181 to the University of California, San Diego. Any errors and opinions are not those of the Army Research Office or Department of Defense and are attributable solely to the author(s). YSJ is grateful for the support received from the American Chemical Society's Petroleum Research Fund (62756-ND5) and the U.S. Department of Energy Office of Science (DE-SC0023390). This article has been authored by an employee of National Technology & Engineering Solutions of Sandia, LLC under Contract No. DE-NA0003525 with the U.S. Department of Energy (DOE). The employee owns all right, title and interest in and to the article and is solely responsible for its contents. The United States Government retains and the publisher, by accepting the article for publication, acknowledges that the United States Government retains a non-exclusive, paid-up, irrevocable, world-wide license to publish or reproduce the published form of this article or allow others to do so, for United States Government purposes. The DOE will provide public access to these results of federally sponsored research in accordance with the DOE Public Access Plan

637 https://www.energy.gov/downloads/doe-public-access-plan. This paper describes objective
638 technical results and analysis. Any subjective views or opinions that might be expressed in the
639 paper do not necessarily represent the views of the U.S. Department of Energy or the United States
640 Government.

641

642 **Author Contributions**

643 The manuscript was written through contributions of all authors. All authors actively edited
644 all draft versions and the final version of the manuscript. AGI proposed the main concept and led
645 the development of the main argument throughout the manuscript; EUB wrote the sections relevant
646 to SiO_2 surface chemistry and specific ion effects; FMG and JMG performed calculations on the
647 ionic strength impacts on the Gouy-Chapman Stern potential and wrote the sections on vSFG and
648 SHG spectroscopies; VHG wrote the sections on complex interfaces with organic species and
649 actively participated in the development of the manuscript structure; YSJ wrote the discussion on
650 nucleation processes in reactive models; NK wrote the section on the variability of adsorption
651 enthalpies with surface coverages; JDK wrote the sections relevant to molecular simulations, and
652 on the new opportunities enabled by exascale computing.

653

654 **Competing interests**

655 The authors declare no competing interests.

656

References

1 Epsztein, R., DuChanois, R. M., Ritt, C. L., Noy, A. & Elimelech, M. Towards single-species selectivity of membranes with subnanometre pores. *Nature Nanotechnology* **15**, 426-436 (2020).

2 Seal, S. *et al.* Engineered defects in cerium oxides: tuning chemical reactivity for biomedical, environmental, & energy applications. *Nanoscale* **12**, 6879-6899 (2020).

3 Jun, Y.-S. Catalyst: The roles of chemistry in clean water for all. *Chem* **9**, 1335-1339 (2023).

4 Gonella, G. *et al.* Water at charged interfaces. *Nature Reviews Chemistry* **5**, 466-485 (2021).

5 Qin, F. & Beckingham, L. E. The impact of mineral reactive surface area variation on simulated mineral reactions and reaction rates. *Applied Geochemistry* **124**, 104852 (2021).

6 Sun, Y. & Li, Y. Application of surface complexation modeling on adsorption of uranium at water-solid interface: A review. *Environmental Pollution* **278**, 116861 (2021).

7 Bañuelos, J. L. *et al.* Oxide–and Silicate–Water Interfaces and Their Roles in Technology and the Environment. *Chemical Reviews* (2023).

8 Xu, T., Zheng, L. & Tian, H. Reactive transport modeling for CO2 geological sequestration. *Journal of Petroleum Science and Engineering*, 765-777 (2011).

9 Li, L. *et al.* Toward catchment hydro-biogeochemical theories. *Wiley Interdisciplinary Reviews: Water* **8**, e1495 (2021).

10 Fischer, C., Arvidson, R. S. & Lüttge, A. How predictable are dissolution rates of crystalline material? *Geochimica et Cosmochimica Acta* (2012).

11 Reeves, D. & Rothman, D. H. Age dependence of mineral dissolution and precipitation rates. *Global biogeochemical cycles* **27**, 906-919 (2013).

12 Zhu, C. *et al.* Testing hypotheses of albite dissolution mechanisms at near-equilibrium using Si isotope tracers. *Geochimica et Cosmochimica Acta* **303**, 15-37 (2021).

13 Schaefer, J., Backus, E. H. & Bonn, M. Evidence for auto-catalytic mineral dissolution from surface-specific vibrational spectroscopy. *Nature Communications* **9**, 3316 (2018).

14 Myalitsin, A., Urashima, S.-H., Nihonyanagi, S., Yamaguchi, S. & Tahara, T. Water structure at the buried silica/aqueous interface studied by heterodyne-detected vibrational sum-frequency generation. *The Journal of Physical Chemistry C* **120**, 9357-9363 (2016).

15 Urashima, S.-h., Myalitsin, A., Nihonyanagi, S. & Tahara, T. The topmost water structure at a charged silica/aqueous interface revealed by heterodyne-detected vibrational sum frequency generation spectroscopy. *The Journal of Physical Chemistry Letters* **9**, 4109-4114 (2018).

16 Khatib, R. *et al.* Water orientation and hydrogen-bond structure at the fluorite/water interface. *Scientific reports* **6**, 1-10 (2016).

17 Rehl, B. *et al.* Water Dipole Populations in the Electrical Double Layer and Their Contributions to the Total Interfacial Potential at Different Surface Charge Densities. (2022).

18 Rehl, B. & Gibbs, J. M. Role of ions on the surface-bound water structure at the silica/water interface: Identifying the spectral signature of stability. *The Journal of Physical Chemistry Letters* **12**, 2854-2864 (2021).

19 Ma, E. *et al.* A new imaginary term in the second-order nonlinear susceptibility from charged interfaces. *The Journal of Physical Chemistry Letters* **12**, 5649-5659 (2021).

20 Brown, M. A. *et al.* Determination of surface potential and electrical double-layer structure at the aqueous electrolyte-nanoparticle interface. *Physical Review X* **6**, 011007 (2016).
21 Dewan, S. *et al.* Structure of water at charged interfaces: A molecular dynamics study. *Langmuir* **30**, 8056-8065 (2014).
22 Piontek, S. M. *et al.* Probing heterogeneous charge distributions at the α-Al2O3 (0001)/H2O interface. *Journal of the American Chemical Society* **142**, 12096-12105 (2020).
23 Lee, S. S., Koishi, A., Bourg, I. C. & Fenter, P. Ion correlations drive charge overscreening and heterogeneous nucleation at solid–aqueous electrolyte interfaces. *Proceedings of the National Academy of Sciences* **118**, e2105154118 (2021).
24 Rashwan, M. *et al.* Structure of the Silica/Divalent Electrolyte Interface: Molecular Insight into Charge Inversion with Increasing pH. *The Journal of Physical Chemistry C* **124**, 26973-26981 (2020).
25 Nakouzi, E. *et al.* Atomic-scale variations of interfacial water structure driven by site-specific chemistry. (2020).
26 Yang, Y., Mayer, K. M., Wickremasinghe, N. S. & Hafner, J. H. Probing the lipid membrane dipole potential by atomic force microscopy. *Biophysical journal* **95**, 5193-5199 (2008).
27 Hapala, P. *et al.* Mapping the electrostatic force field of single molecules from high-resolution scanning probe images. *Nature communications* **7**, 1-8 (2016).
28 Bonagiri, L. K. S. *et al.* Real-space charge density profiling of electrode–electrolyte interfaces with angstrom depth resolution. *ACS nano* **16**, 19594-19604 (2022).
29 Nakouzi, E. *et al.* Moving beyond the Solvent-Tip Approximation to Determine Site-Specific Variations of Interfacial Water Structure through 3D Force Microscopy. *The Journal of Physical Chemistry C* **125**, 1282-1291 (2021). https://doi.org:10.1021/acs.jpcc.0c07901
30 Sayle, T. X. *et al.* Structure–activity map of ceria nanoparticles, nanocubes, and mesoporous architectures. *Chemistry of Materials* **28**, 7287-7295 (2016).
31 Ong, S., Zhao, X. & Eisenthal, K. B. Polarization of water molecules at a charged interface: second harmonic studies of the silica/water interface. *Chemical Physics Letters* **191**, 327-335 (1992).
32 Azam, M. S., Weeraman, C. N. & Gibbs-Davis, J. M. Specific cation effects on the bimodal acid–base behavior of the silica/water interface. *The journal of physical chemistry letters* **3**, 1269-1274 (2012).
33 Darlington, A. M. & Gibbs-Davis, J. M. Bimodal or trimodal? The influence of starting pH on site identity and distribution at the low salt aqueous/silica interface. *The Journal of Physical Chemistry C* **119**, 16560-16567 (2015).
34 Gibbs-Davis, J. M., Kruk, J. J., Konek, C. T., Scheidt, K. A. & Geiger, F. M. Jammed acid− base reactions at interfaces. *Journal of the American Chemical Society* **130**, 15444-15447 (2008).
35 Jun, Y.-S. *et al.* Classical and Nonclassical Nucleation and Growth Mechanisms for Nanoparticle Formation. *Annual Review of Physical Chemistry* **73**, 453-477 (2022).
36 Jun, Y. S., Kim, D. & Neil, C. W. Heterogeneous Nucleation and Growth of Nanoparticles at Environmental Interfaces. *Accounts of Chemical Research* **49**, 1681-1690 (2016).
37 Isaienko, O. & Borguet, E. Hydrophobicity of hydroxylated amorphous fused silica surfaces. *Langmuir* **29**, 7885-7895 (2013).
38 Cyran, J. D. *et al.* Molecular hydrophobicity at a macroscopically hydrophilic surface. *Proceedings of the national academy of sciences* **116**, 1520-1525 (2019).

39 Leung, K., Nielsen, I. M. & Criscenti, L. J. Elucidating the bimodal acid− base behavior of the water− silica interface from first principles. *Journal of the American Chemical Society* **131**, 18358-18365 (2009).
40 Pfeiffer-Laplaud, M., Costa, D., Tielens, F., Gaigeot, M.-P. & Sulpizi, M. Bimodal acidity at the amorphous silica/water interface. *The Journal of Physical Chemistry C* **119**, 27354-27362 (2015).
41 Wagner, M., Meyer, B., Setvin, M., Schmid, M. & Diebold, U. Direct assessment of the acidity of individual surface hydroxyls. *Nature* **592**, 722-725 (2021).
42 Macias-Romero, C., Nahalka, I., Okur, H. I. & Roke, S. Optical imaging of surface chemistry and dynamics in confinement. *Science* **357**, 784-788 (2017).
43 Kwon, K. D., Vadillo-Rodriguez, V., Logan, B. E. & Kubicki, J. D. Interactions of biopolymers with silica surfaces: Force measurements and electronic structure calculation studies. *Geochimica et Cosmochimica Acta* **70**, 3803-3819 (2006).
44 DeWalt-Kerian, E. L. *et al.* pH-dependent inversion of Hofmeister trends in the water structure of the electrical double layer. *The journal of physical chemistry letters* **8**, 2855-2861 (2017).
45 Schwierz, N., Horinek, D., Sivan, U. & Netz, R. R. Reversed Hofmeister series—The rule rather than the exception. *Current opinion in colloid & interface science* **23**, 10-18 (2016).
46 Ilgen, A. G., Leung, K., Criscenti, L. J. & Greathouse, J. A. Adsorption at Nanoconfined Solid–Water Interfaces. *Annual Review of Physical Chemistry* (2023).
47 Sit, I., Wu, H. & Grassian, V. H. Environmental Aspects of Oxide Nanoparticles: Probing Oxide Nanoparticle Surface Processes Under Different Environmental Conditions. *Annual Review of Analytical Chemistry* **14**, 489-514 (2021).
48 Ilgen, A. G. *et al.* Defining silica–water interfacial chemistry under nanoconfinement using lanthanides. *Environmental Science: Nano* **8**, 432-443 (2021).
49 Zhu, Y. *et al.* Ionic surface propensity controls pH in nanopores. *Chem* **8**, 1-15 (2022).
50 Azam, S., Darlington, A. & Gibbs-Davis, J. M. The influence of concentration on specific ion effects at the silica/water interface. *Journal of Physics: Condensed Matter* **26**, 244107 (2014).
51 Konek, C. T. *et al.* Interfacial acidities, charge densities, potentials, and energies of carboxylic acid-functionalized silica/water interfaces determined by second harmonic generation. *Journal of the American Chemical Society* **126**, 11754-11755 (2004).
52 Gershevitz, O. & Sukenik, C. N. In situ FTIR-ATR analysis and titration of carboxylic acid-terminated SAMs. *Journal of the American Chemical Society* **126**, 482-483 (2004).
53 Winter, N., Vieceli, J. & Benjamin, I. Hydrogen-bond structure and dynamics at the interface between water and carboxylic acid-functionalized self-assembled monolayers. *The Journal of Physical Chemistry B* **112**, 227-231 (2008).
54 Jordan, D. S., Saslow, S. A. & Geiger, F. M. Exponential sensitivity and speciation of Al (III), Sc (III), Y (III), La (III), and Gd (III) at fused silica/water interfaces. *The Journal of Physical Chemistry A* **115**, 14438-14445 (2011).
55 Malin, J. N., Holland, J. G. & Geiger, F. M. Free energy relationships in the electric double layer and alkali earth speciation at the fused silica/water interface. *The Journal of Physical Chemistry C* **113**, 17795-17802 (2009).
56 Criscenti, L. J. & Sverjensky, D. A. The role of electrolyte anions (ClO 4-, NO 3-, and Cl-) in divalent metal (M 2+) adsorption on oxide and hydroxide surfaces in salt solutions. *American Journal of Science* **299**, 828-899 (1999).
57 Zhang, Z. *et al.* Structure of hydrated Zn2+ at the rutile TiO2 (110)-aqueous solution interface: Comparison of X-ray standing wave, X-ray absorption spectroscopy, and density functional theory results. *Geochimica et Cosmochimica Acta* **70**, 4039-4056 (2006).

58 Soderholm, L., Skanthakumar, S. & Wilson, R. E. Structures and energetics of erbium chloride complexes in aqueous solution. *The Journal of Physical Chemistry A* **113**, 6391-6397 (2009).
59 Dove, P. M. The dissolution kinetics of quartz in sodium chloride solutions at 25 degrees to 300 degrees C. *American Journal of Science* **294**, 665 (1994). https://doi.org:10.2475/ajs.294.6.665
60 Icenhower, J. P. & Dove, P. M. The dissolution kinetics of amorphous silica into sodium chloride solutions: effects of temperature and ionic strength. *Geochimica et Cosmochimica Acta* **64**, 4193-4203 (2000).
61 Kubicki, J. D., Sofo, J. O., Skelton, A. A. & Bandura, A. V. A new hypothesis for the dissolution mechanism of silicates. *The Journal of Physical Chemistry C* **116**, 17479-17491 (2012).
62 Dewan, S., Yeganeh, M. S. & Borguet, E. Experimental correlation between interfacial water structure and mineral reactivity. *The Journal of Physical Chemistry Letters* **4**, 1977-1982 (2013).
63 Li, Q. & Jun, Y.-S. Salinity-Induced Reduction of Interfacial Energies and Kinetic Factors during Calcium Carbonate Nucleation on Quartz. *The Journal of Physical Chemistry C* **123**, 14319-14326 (2019).
64 Jun, Y. S., Lee, B. & Waychunas, G. A. In situ observations of nanoparticle early development kinetics at mineral-water interfaces. *Environmental Science and Technology* **44**, 8182-8189 (2010).
65 Neil, C. W., Lee, B. & Jun, Y. S. Different Arsenate and Phosphate Incorporation Effects on the Nucleation and Growth of Iron(III) (Hydr)oxides on Quartz. *Environmental Science & Technology* **48**, 11883-11891 (2014).
66 Ray, J. R., Lee, B., Baltrusaitis, J. & Jun, Y. S. Formation of Iron(III) Hydroxides on Polyaspartate- and Alginate-Coated SiO_2: Effects of Substrate Hydrophilicity and Functional Groups at the Surface. *Environ. Sci. Technol.* **46**, 13167-13175 (2012).
67 Li, Q., Steefel, C. I. & Jun, Y. S. Incorporating Nanoscale Effects into a Continuum-Scale Reactive Transport Model for CO2-Deteriorated Cement. *Envir. Sci. & Tech.* **51**, 10861-10871 (2017).
68 Hu, Y., Lee, B., Bell, C. & Jun, Y. S. Environmentally abundant anions influence the nucleation, growth, ostwald ripening, and aggregation of hydrous Fe(III) oxides. *Langmuir* **28**, 7737-7746 (2012).
69 Givens, B. E., Diklich, N. D., Fiegel, J. & Grassian, V. H. Adsorption of bovine serum albumin on silicon dioxide nanoparticles: Impact of pH on nanoparticle–protein interactions. *Biointerphases* **12**, 02D404 (2017).
70 Xu, Z. & Grassian, V. H. Bovine Serum Albumin Adsorption on TiO2 Nanoparticle Surfaces: Effects of pH and Coadsorption of Phosphate on Protein–Surface Interactions and Protein Structure. *The Journal of Physical Chemistry C* **121**, 21763-21771 (2017).
71 Ustunol, I. B., Coward, E. K., Quirk, E. & Grassian, V. H. Interaction of beta-lactoglobulin and bovine serum albumin with iron oxide (α-Fe2O3) nanoparticles in the presence and absence of pre-adsorbed phosphate. *Environmental Science: Nano* **8**, 2811-2823 (2021).
72 Kim, D. & Grassian, V. H. Attenuated Total Reflection-Fourier Transform Infrared and Atomic Force Microscopy-Infrared Spectroscopic Investigation of Suwannee River Fulvic Acid and Its Interactions with α-FeOOH. *ACS Earth and Space Chemistry* **6**, 81-89 (2021).
73 Jayalath, S., Wu, H., Larsen, S. C. & Grassian, V. H. Surface adsorption of Suwannee River humic acid on TiO2 nanoparticles: a study of pH and particle size. *Langmuir* **34**, 3136-3145 (2018).

74 Wheeler, K. E. *et al.* Environmental dimensions of the protein corona. *Nature Nanotechnology* **16**, 617-629 (2021).
75 Mauvisseau, Q. *et al.* The multiple states of environmental DNA and what is known about their persistence in aquatic environments. *Environmental Science & Technology* **56**, 5322-5333 (2022).
76 DelloStritto, M., Piontek, S. M., Klein, M. L. & Borguet, E. Relating interfacial order to sum frequency generation with Ab initio simulations of the aqueous Al2O3 (0001) and (1120) interfaces. *The Journal of Physical Chemistry C* **122**, 21284-21294 (2018).
77 Tuladhar, A. *et al.* Ions tune interfacial water structure and modulate hydrophobic interactions at silica surfaces. *Journal of the American Chemical Society* **142**, 6991-7000 (2020).
78 Yalcin, S. E., Legg, B. A., Yeşilbaş, M., Malvankar, N. S. & Boily, J.-F. Direct observation of anisotropic growth of water films on minerals driven by defects and surface tension. *Science advances* **6**, eaaz9708 (2020).
79 Le Traon, C., Aquino, T., Bouchez, C., Maher, K. & Le Borgne, T. Effective kinetics driven by dynamic concentration gradients under coupled transport and reaction. *Geochimica et Cosmochimica Acta* **306**, 189-209 (2021).
80 Bakaev, V., Bakaeva, T. & Pantano, C. On inverse adsorption chromatography. 2. Determination of isotherms and heats of adsorption as well as energy distributions of adsorption sites. *The Journal of Physical Chemistry C* **111**, 7473-7486 (2007).
81 Criscenti, L. J. & Sverjensky, D. A. A single-site model for divalent transition and heavy metal adsorption over a range of metal concentrations. *Journal of colloid and interface science* **253**, 329-352 (2002).
82 Kubicki, J. D., Kabengi, N., Chrysochoou, M. & Bompoti, N. Density functional theory modeling of chromate adsorption onto ferrihydrite nanoparticles. *Geochemical transactions* **19**, 1-12 (2018).
83 Kabengi, N. J., Chrysochoou, M., Bompoti, N. & Kubicki, J. D. An integrated flow microcalorimetry, infrared spectroscopy and density functional theory approach to the study of chromate complexation on hematite and ferrihdyrite. *Chemical Geology* **464**, 23-33 (2017).
84 Bompoti, N. M., Chrysochoou, M. & Machesky, M. L. A unified surface complexation modeling approach for chromate adsorption on iron oxides. *Environmental science & technology* **53**, 6352-6361 (2019).
85 Livi, K. J., Villalobos, M., Ramasse, Q., Brydson, R. & Salazar-Rivera, H. S. Surface Site Density of Synthetic Goethites and Its Relationship to Atomic Surface Roughness and Crystal Size. *Langmuir* **39**, 556-562 (2022).
86 Li, Q. & Jun, Y.-S. The apparent activation energy and pre-exponential kinetic factor for heterogeneous calcium carbonate nucleation on quartz. *Communications Chemistry* **1**, 56 (2018).
87 Li, Q., Fernandez-Martinez, A., Lee, B., Waychunas, G. A. & Jun, Y.-S. Interfacial energies for heterogeneous nucleation of calcium carbonate on mica and quartz. *Environmental science & technology* **48**, 5745-5753 (2014).
88 Neil, C. W. & Jun, Y. S. Fe^{3+} Addition Promotes Arsenopyrite Dissolution and Iron(III) (Hydr)oxide Formation and Phase Transformation. *Environmental Science & Technology Letters* **3**, 30-35 (2016).
89 Neil, C. W., Yang, Y. J., Schupp, D. & Jun, Y. S. Water Chemistry Impacts on Arsenic Mobilization from Arsenopyrite Dissolution and Secondary Mineral Precipitation: Implications for Managed Aquifer Recharge. *Environmental Science & Technology* **48**, 4395-4405 (2014).

90 Wu, X., Bowers, B., Kim, D., Lee, B. & Jun, Y.-S. Dissolved Organic Matter Affects Arsenic Mobility and Iron(III) (hydr)oxide Formation: Implications for Managed Aquifer Recharge. *Environmental Science & Technology* **53**, 14357-14367 (2019).
91 Wu, X. *et al.* Effects of Phosphate, Silicate, and Bicarbonate on Arsenopyrite Dissolution and Secondary Mineral Precipitation. *ACS Earth and Space Chemistry* **4**, 515-525 (2020).
92 Lutzenkirchen, J. *Surface complexation modelling*. (Elsevier, 2006).
93 Metropolis, N. & Ulam, S. The monte carlo method. *Journal of the American statistical association* **44**, 335-341 (1949).
94 Jansen, A. P. J. *An introduction to kinetic Monte Carlo simulations of surface reactions*. Vol. 856 (Springer, 2012).
95 Zhang, L. & Lüttge, A. Aluminosilicate dissolution kinetics: a general stochastic model. *The Journal of Physical Chemistry B* **112**, 1736-1742 (2008).
96 Kurganskaya, I. & Luttge, A. Kinetic Monte Carlo simulations of silicate dissolution: model complexity and parametrization. *The Journal of Physical Chemistry C* **117**, 24894-24906 (2013).
97 Pedrosa, T., Kurganskaya, I., Fischer, C. & Luttge, A. A statistical approach for analysis of dissolution rates including surface morphology. *Minerals* **9**, 458 (2019).
98 Luttge, A., Arvidson, R. S., Fischer, C. & Kurganskaya, I. Kinetic concepts for quantitative prediction of fluid-solid interactions. *Chemical Geology* **504**, 216-235 (2019).
99 Guren, M. G., Renard, F. & Noiriel, C. Dissolution rate variability at carbonate surfaces: 4D X-ray micro-tomography and stochastic modeling investigations. *Frontiers in Water* **5**, 1185608 (2023).
100 Karimzadeh, L. & Fischer, C. Implementing heterogeneous crystal surface reactivity in reactive transport simulations: The example of calcite dissolution. *ACS Earth and Space Chemistry* **5**, 2408-2418 (2021).
101 Schabernack, J. & Fischer, C. Improved kinetics for mineral dissolution reactions in pore-scale reactive transport modeling. *Geochimica et Cosmochimica Acta* **334**, 99-118 (2022).
102 Cygan, R. T. Molecular modeling in mineralogy and geochemistry. *Molecular Modeling Theory: Applications in the Geosciences* **42**, 1-35 (2001).
103 Montes de Oca Zapiain, D., Wood, M., Sema, D. & Thompson, A. Optimal Development of Transferable Machine Learning Interatomic Potentials using Active Learning. *Bulletin of the American Physical Society* (2023).
104 Akai, T., Blunt, M. J. & Bijeljic, B. Pore-scale numerical simulation of low salinity water flooding using the lattice Boltzmann method. *Journal of colloid and interface science* **566**, 444-453 (2020).
105 Fitts, J. P. *et al.* Second-harmonic generation and theoretical studies of protonation at the water/α-TiO2 (1 1 0) interface. *Chemical Physics Letters* **411**, 399-403 (2005).
106 Zhong, S. *et al.* Machine learning: new ideas and tools in environmental science and engineering. *Environmental Science & Technology* **55**, 12741-12754 (2021).